Received: 10 August 2021 | Revised: 12 November 2021 | Accepted: 30 November 2021

DOI: 10.1096/fj.202101262R

THE FASEB JOURNAL

RESEARCH ARTICLE

Short-term tetrabromobisphenol A exposure promotes fibrosis of human uterine fibroid cells in a 3D culture system through TGF-beta signaling

Jingli Liu[1] | **Linda Yu**[1] | **Lysandra Castro**[1] | **Yitang Yan**[1] | **Natasha P. Clayton**[2] | **Pierre Bushel**[3] | **Norris D. Flagler**[2] | **Erica Scappini**[4] | **Darlene Dixon**[1]

[1]Mechanistic Toxicology Branch (MTB), Division of the National Toxicology Program (DNTP), National Institute of Environmental Health Sciences (NIEHS), NIH, Research Triangle Park, North Carolina, USA

[2]Cellular & Molecular Pathogenesis Branch, DNTP NIEHS, NIH, Research Triangle Park, North Carolina, USA

[3]Biostatistics & Computational Biology Branch, Division of Intramural Research (DIR), NIEHS, NIH, Research Triangle Park, North Carolina, USA

[4]Signal Transduction Laboratory, DIR, NIEHS, NIH, Research Triangle Park, North Carolina, USA

Correspondence
Darlene Dixon, Molecular Pathogenesis Group, MTB, NIEHS, NIH, 111 T.W. Alexander Drive, Building 101, South Campus, Research Triangle Park, NC 27709, USA.
Email: dixon@niehs.nih.gov

Funding information
HHS | National Institutes of Health (NIH), Grant/Award Number: ES021196-27

Abstract

Tetrabromobisphenol A (TBBPA), a derivative of BPA, is a ubiquitous environmental contaminant with weak estrogenic properties. In women, uterine fibroids are highly prevalent estrogen-responsive tumors often with excessive accumulation of extracellular matrix (ECM) and may be the target of environmental estrogens. We have found that BPA has profibrotic effects in vitro, in addition to previous reports of the in vivo fibrotic effects of BPA in mouse uterus. However, the role of TBBPA in fibrosis is unclear. To investigate the effects of TBBPA on uterine fibrosis, we developed a 3D human uterine leiomyoma (ht-UtLM) spheroid culture model. Cell proliferation was evaluated in 3D ht-UtLM spheroids following TBBPA (10^{-6}–200 μM) administration at 48 h. Fibrosis was assessed using a Masson's Trichrome stain and light microscopy at 7 days of TBBPA (10^{-3} μM) treatment. Differential expression of ECM and fibrosis genes were determined using RT² Profiler™ PCR arrays. Network and pathway analyses were conducted using Ingenuity Pathway Analysis. The activation of pathway proteins was analyzed by a transforming growth factor-beta (TGFB) protein array. We found that TBBPA increased cell proliferation and promoted fibrosis in 3D ht-UtLM spheroids with increased deposition of collagens. TBBPA upregulated the expression of profibrotic genes and corresponding proteins associated with the TGFB pathway. TBBPA activated TGFB signaling through phosphorylation of TGFBR1 and downstream effectors—small mothers against decapentaplegic -2 and -3 proteins (SMAD2 and SMAD3). The 3D ht-UtLM spheroid model is an effective system for

Abbreviations: *ADAMTS8*, ADAM metallopeptidase with thrombospondin type 1 motif 8; ANOVA, one-way analysis of variance; BFR, brominated flame retardant; CCK8, Cell Counting Kit 8; *CDH1*, cadherin 1; *COL1A1*, collagen type I alpha 1 chain; Co-SMADs, common-partner SMADs; ECM, extracellular matrix; H&E, hematoxylin and eosin; ht-UtLM, Human uterine leiomyoma cell line immortalized via retroviral transfection of telomerase; IPA, Ingenuity Pathway Analysis; I-SMADs, inhibitory SMADs; *ITGAM*, integrin subunit alpha M; *MMP8*, matrix metallopeptidase 8; NBF, neutral buffered formalin; *PPAR*, peroxisome proliferator activated receptor; R-SMADs, receptor-regulated SMADs; *SELL*, selectin L; SMAD, mothers against decapentaplegic; TBBPA, Tetrabromobisphenol A; TGFB, transforming growth factor beta; TGFBR, transforming growth factor beta receptor.

This is an open access article under the terms of the Creative Commons Attribution NonCommercial License, which permits use, distribution and reproduction in any medium, provided the original work is properly cited and is not used for commercial purposes.
Published 2022. This article is a U.S. Government work and is in the public domain in the USA. *The FASEB Journal* published by Wiley Periodicals LLC on behalf of Federation of American Societies for Experimental Biology.

studying environmental agents on human uterine fibrosis. TBBPA can promote fibrosis in uterine fibroid through TGFB/SMAD signaling.

KEYWORDS
extracellular matrix, fibrosis, tetrabromobisphenol A, TGFB, uterine fibroid

1 | INTRODUCTION

Tetrabromobisphenol A [TBBPA, 4,4′-isopropylidenebis (2,6-dibromophenol)] is a persistent and prevalent contaminant in the environment, mainly used as a brominated flame retardant (BFR) in epoxy and polycarbonate resins.[1] The largest production volume of BFRs, globally, is estimated at over 145 000 tons per year.[2] TBBPA readily bioaccumulates due to its chemical properties of high lipophilicity, low volatility, and low water solubility, which leads to environmental persistence in dust, soil, sediments, and accumulation in plants, humans, and wildlife.[3,4] TBBPA has been detected in the serum of women in Korea ranging at 0.05–74 ng/g lipid weight,[5] and in human milk ranging from <0.03 to 37.3 ng/g lipid weight in the United States, France, Japan, and China.[6] The widespread use of TBBPA, its environmental persistence and potential toxicity, and particularly its endocrine-disrupting effects have focused extensive concern on its possible adverse health risks for wildlife and humans.

TBBPA is a four-meta-brominated derivative of BPA and has been shown to have weak estrogenic activity.[7] TBBPA and BPA have similar structures and share some common characteristics or activities (Figure S1). TBBPA can bind to the classical estrogen receptors but to a lesser extent than BPA.[8,9] TBBPA at doses of 1 to 10 μM can induce cell proliferation in a human estrogen-sensitive breast cancer cell line, MCF-7.[8] TBBPA administration by intraperitoneal injection has been shown to increase uterine weight in a uterotrophic assay in ovariectomized mice.[7]

It has been reported that TBBPA exposure can disrupt the endocrine, reproductive, and immune systems in addition to neurobehavioral functions in animals.[1,10–12] In a 2-year bioassay of chronic TBBPA exposure in female Wistar Han rats conducted by the National Toxicology Program (NTP), the association between TBBPA exposure and increased incidence of benign and malignant uterine tumors was found.[13] Increased incidences of nonneoplastic lesions of the uterus (predominately atypical endometrial hyperplasia) and rete ovarii cysts in female Wistar Han rats were also induced by TBBPA.[13] Whether TBBPA affects growth or induces fibrosis in the uterus has not been reported, although there are numerous reports of fibrosis in the uterus, heart, and liver of rodents following the administration of BPA.[14–17]

Uterine leiomyomas, also called uterine fibroids, are benign smooth muscle tumors commonly diagnosed in reproductive-aged women,[18] that are characterized by progressive fibrosis due to excessive extracellular matrix (ECM) accumulation.[19] As the most common gynecologic neoplasms, uterine fibroids can have a cumulative incidence of nearly 70% in Caucasian women and >80% in Black women by age 50.[20] Although nonsurgical treatments can be used to help control the symptoms of uterine fibroids, hysterectomy is currently the only essentially curative treatment that prevents recurrence.[21] However, this poses risks associated with surgery or possible post-surgical complications and leads to a high economic burden. Uterine fibroid tumors are estrogen responsive; therefore, it is important to investigate potential environmental or endocrine-disrupting factors and their molecular mechanisms, by which they may contribute to fibroid development and growth, and to explore measures to prevent these exposures.

Understanding the molecular mechanisms of uterine leiomyoma development requires in vitro models that closely mimic the in vivo tumors in humans. Therefore, in this study, a three-dimensional (3D) human uterine leiomyoma (ht-UtLM) cell model was developed and used to explore the effects of TBBPA on fibrosis development.

2 | MATERIALS AND METHODS

2.1 | Development of 3D culture system

The immortalized UtLM-hTERT (ht-UtLM) cells established in our laboratory were used to develop a 3D culture model.[22] Ht-UtLM cells were seeded in 96-well ultra-low attachment plates (Corning, US) and maintained in mesenchymal stem cell growth medium (MSCGM; Lonza, US) at 37°C and 5% CO_2 atmosphere.[23] For each well, 5×10^4 cells were seeded and formed one spheroid. Half of the medium was replaced every 2 days. At day 4 after seeding and spheroid formation, the 3D ht-UtLM cultures were treated with 10^{-6}–200 μM TBBPA. DMSO 0.1% was used as a vehicle control.

2.2 | Histology analysis

The collection of spheroids and paraffin embedding were conducted following techniques developed in our laboratory.[24] Briefly, ht-UtLM spheroids with or without TBBPA

treatment at 10^{-3} μM ($n = 48$ for each group) were collected in a microcentrifuge tube and fixed in 10% neutral buffered formalin (NBF) for 10 min. Then 1% agarose solution (Agarose I, VWR Corporation, USA) was added, mixed gently with spheroids, and allowed to solidify for about 1 h at room temperature. The agarose gel with spheroids were sliced longitudinally and processed on a tissue processor (Leica ASP6025, Germany) prior to embedding in paraffin. Sections were cut at 5 μm for hematoxylin and eosin (H&E) and Masson's Trichrome staining. The Masson's Trichrome stain stained the collagen blue and smooth muscle (fibroid cells) stained red. Image analysis was performed using an Aperio colocalization algorithm as previously reported.[25] The collagen content was expressed as the percentage of collagen present in each spheroid.

2.3 | Cell proliferation assay

Cell proliferation of ht-UtLM spheroids treated with TBBPA (10^{-6}–200 μM) was evaluated using a Cell Counting Kit 8 (CCK8) (Sigma-Aldrich, US) at 48 h. The absorbance at 450 nm was measured by a microplate reader (SpectraMax M5, US). There were eight spheroids for each group and the experiments were repeated three times.

2.4 | RT^2 profiler PCR array

RNA was extracted from spheroids ($n = 96$ for each group) with or without TBBPA treatment at 10^{-3} μM for 24 h using RNeasy Mini Kit (Qiagen, US) and then purified followed by reverse-transcription to cDNA using cDNA RT^2 First Strand Kit (Qiagen, US). RT^2 profiler PCR arrays were conducted using human Extracellular Matrix and Adhesion Molecules array kit (Qiagen, PAHS-013Z) and human Fibrosis array kit (Qiagen, PAHS-120Z). Real-time PCR was run on ABI Quantstudio 7 Flex (ThermoFisher Scientific, US). For each array, there were 84 related genes and three replicates of samples for each group. The data were analyzed by RT^2 profiler PCR array analysis tool and Ingenuity Pathway Analysis (IPA, Qiagen, US).

2.5 | Protein extraction

Protein was extracted from ht-UtLM spheroids ($n = 96$ for each group) with RIPA lysis buffer and homogenized using an ultrasonic homogenizer. Sonication duration was 60–90 s at an ultrasonic cycle mode of 15 s sonication and 10 s resting time. The samples were kept on ice all the times. The lysate was centrifuged, and the supernatant was collected. Protein concentrations were determined by a Pierce protein assay BCA.

2.6 | TGFB phospho-protein array

Protein extractions from ht-UtLM spheroids with or without TBBPA treatment at 10^{-3} μM for 3 h were used to conduct TGFB phospho-protein array analysis (Full Moon Biosystems, cat# PTG176, US), with each array containing 176 specific phosphorylation antibodies for the TGFB signaling pathway. There were six replicates for each antibody. The array was conducted following the manufacturer's instructions. The slides were scanned by Agilent Technologies Microarray scanner and the signal intensity was determined using GenePix Pro Image software. Data analysis was performed with IPA software (Qiagen, US).

2.7 | Western blot analysis

Protein extractions and western blotting were performed to determine the protein expression of PCNA in ht-UtLM spheroids with or without TBBPA treatment at 10^{-3} μM for 7 days. The primary antibody mouse monoclonal anti-PCNA (#2586, Cell Signaling) was used at 1:2000 dilution over night at 4°C. Secondary antibody anti-mouse IgG horseradish peroxidase linked (A931V, GE Healthcare) was used at 1:5000. The detection kit used was the ECL Western Blotting Detection Reagent (#RPn2106, GE Healthcare). Band intensity was quantified by Fiji.

2.8 | Pathway and network analysis by IPA

The list of differentially expressed genes in the RT^2 profiler PCR arrays and phosphorylated proteins in TGFB phospho-protein array, containing gene identifiers and corresponding expression values, was uploaded into the IPA software (Qiagen, US). The "core analysis" was used to interpret the differentially expressed data, which included canonical pathways, upstream regulators, associated diseases and functions, as well as molecule networks.

2.9 | Statistical analysis

Results were expressed as mean ± SE from at least three replicates. The statistical significance of the differences was determined by *t*-test or one-way analysis of variance (ANOVA) followed by Dunnett's post hoc comparisons test. Statistical significance was defined as $p < .05$.

3 | RESULTS

3.1 | Development of 3D ht-UtLM spheroid culture model

One of the advantages of 3D culture system compared to 2D cell system is to closely mimic in vivo tumors. Therefore, a 3D human fibroid spheroid model was developed in this study. As early as day 2 after seeding, the ht-UtLM cells self-aggregated to form spheroids. The 3D ht-UtLM spheroids could be maintained for at least 3 weeks in culture. Compared to the 2D cells, the 3D spheroids had similar morphology to in vivo fibroids, consisting of typical smooth muscle cells and extracellular matrix (Figure 1A,B). There was minimal collagen deposition in 2D cell cultures (<1%), while it was clearly present in 3D spheroids by day 7 (40%–70%), which is similar to the abundant and predominant collagen accumulation in mid-late phases (phase 3 10%–50% and phase 4 >50%) of human uterine fibroid tissues.[26]

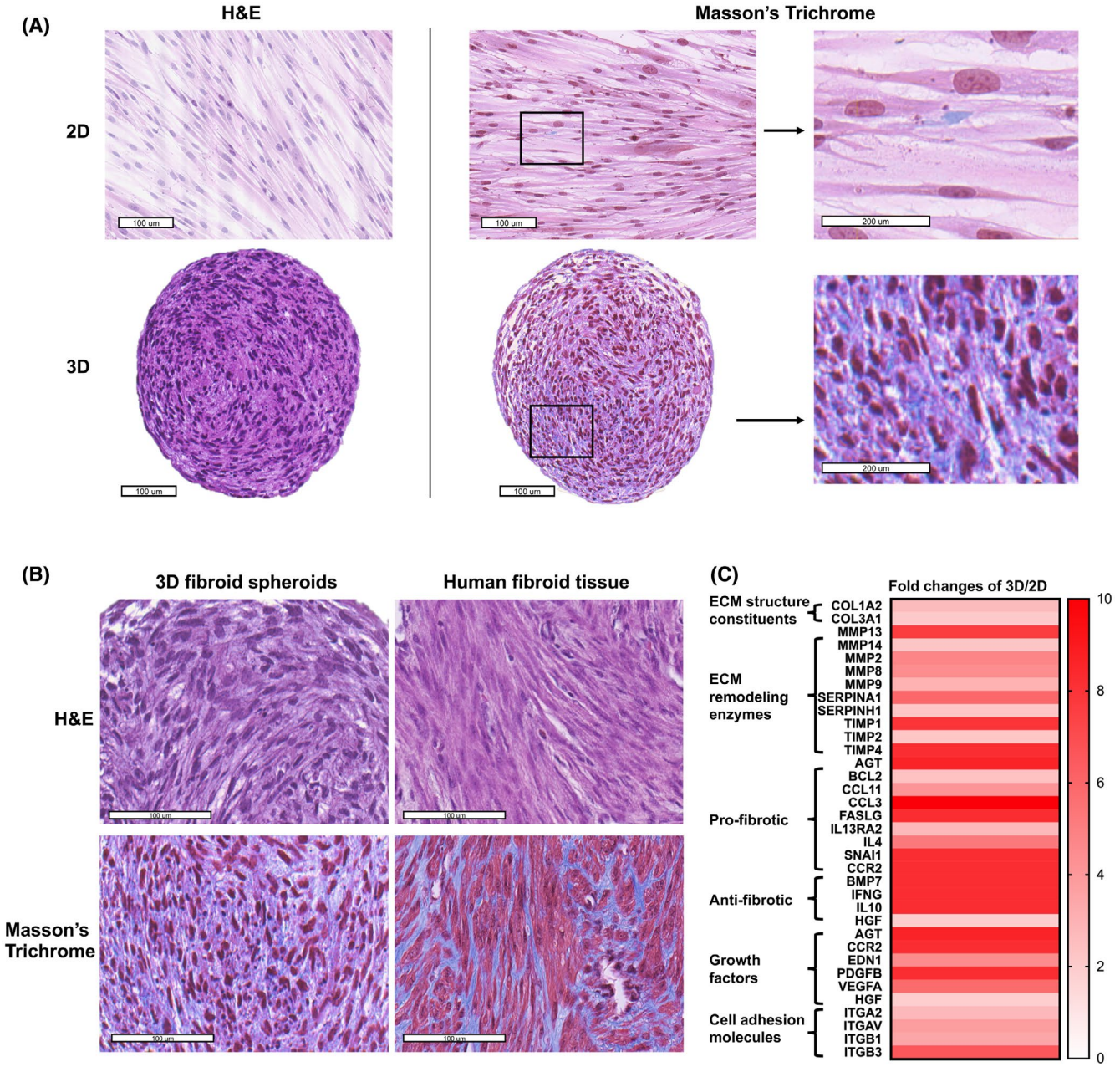

FIGURE 1 Histology and morphology of ht-UtLM cells on day 7 in 2D and 3D cultures as well as human uterine fibroid tissues. (A) Morphology of ht-UtLM cells in 2D and 3D cultures. Hematoxylin and eosin (H&E) staining (left); Masson's Trichrome staining (right). Blue color indicates collagen. (B) Morphology of 3D ht-UtLM spheroids and primary human fibroid tissues. (C) Heat map of ECM and fibrosis-associated gene expression in 3D compared to 2D by Fibrosis RT^2 profiler PCR array. Fold change >2 and $p < .05$. Scale bar = 100 μm

The comparison of basal ECM and fibrosis-associated genes that were significantly differentially expressed between 2D and 3D cells ($p < .05$) was evaluated using Fibrosis RT^2 Profiler PCR arrays (Figure 1C). Compared to 2D cells, the 3D spheroids showed increased collagens and ECM remodeling enzymes including both metalloproteinases and their peptidase inhibitors, as well as pro- and antifibrotic genes, all of which indicated enhanced ECM dynamics of matrix production and degradation. Also, growth factor genes and cell adhesion molecules were also increased in 3D spheroids. These findings indicated that the association of cells in a 3D configuration stimulated a microenvironment that kept cells in an active status and resulted in cell growth and ECM production, commonly observed in uterine fibroid tumors in vivo.

3.2 | Proliferative effects of TBBPA in 3D ht-UtLM spheroids

To evaluate the effects of TBBPA on cell proliferation of 3D ht-UtLM spheroids, the 3D ht-UtLM spheroids were treated with TBBPA ranging from 10^{-6} to 200 μM starting at day 4 after seeding. Cell proliferation was evaluated by CCK8 after treatment for 48 h. As shown in Figure 2, TBBPA increased cell proliferation significantly ($p < .05$) starting from 10^{-3} to 1 μM, and decreased cell proliferation at high concentrations of 100 μM or 200 μM. Therefore, we chose the lowest human relevant concentration, 10^{-3} μM,[27] that could induce significant proliferative effects in ht-UtLM spheroids to further evaluate if this concentration of TBBPA could also elicit a fibrotic effect.

3.3 | Profibrotic effects of TBBPA in 3D ht-UtLM spheroids

After the administration of TBBPA at 10^{-3} μM for 24 h, ECM RT^2 Profiler PCR arrays were conducted to investigate the effect of TBBPA on the expression of ECM genes. A heat map of gene expression data showed 11 out of 84 ECM genes were significantly regulated (fold change >2 and $p < .05$) (Figure 3A), especially several collagen subtype genes (*COL1A1*, *COL5A1*, *COL6A1*, *COL12A1*, *COL15A1*, and *COL16A1*) were upregulated significantly with TBBPA treatment (Figure 3B). In addition, metalloproteinase genes *ADAMTS8* and *MMP8* which function to degrade ECM[28] were downregulated (Figure 3A). *CDH1*, *ITGAM*, and *SELL* genes involved in cell adhesion were also downregulated, which could also affect tissue remodeling and ECM balance (Figure 3A). This indicated that TBBPA could increase gene expression of molecules important in ECM production and downregulate those involved in the breakdown of ECM components or in tissue remodeling.

At the protein level, there was an increased percent collagen accumulation in 3D ht-UtLM spheroids in the TBBPA-treated group compared to control as evidenced with a Masson's Trichrome stain (Figure 4A,B) ($p < .05$). The diameter of spheroids was also increased by TBBPA exposure compared to controls at day 7 (Figure 4C) ($p < .05$), which was at least in part dependent on collagen accumulation, in addition to increased fibroid cell proliferation with higher expression of PCNA (Figure 4D) and increased cell number (Figure 2). The above data demonstrated that TBBPA could promote ECM production in 3D ht-UtLM spheroids.

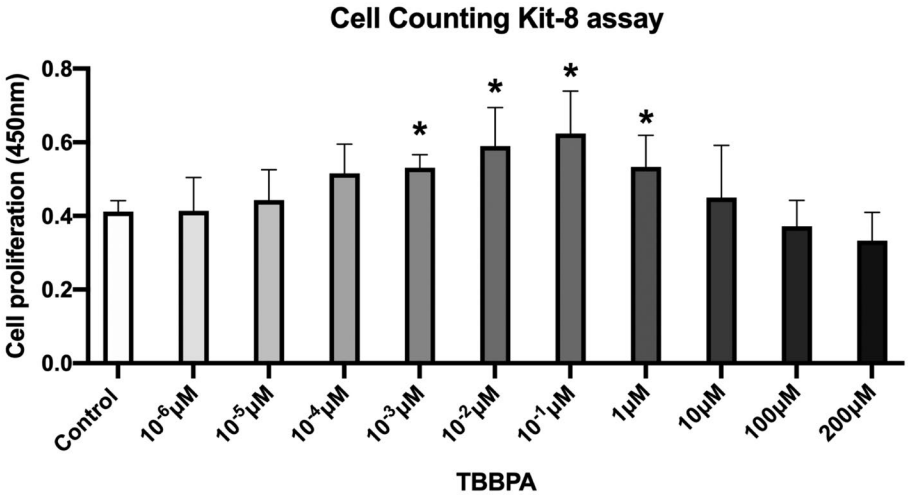

FIGURE 2 Cell proliferation of ht-UtLM spheroids by Cell Counting Kit (CCK8) assay. The ht-UtLM spheroids were treated with TBBPA at different concentrations (10^{-6}–200 μM) for 48 h. *$p < .05$ compared to control

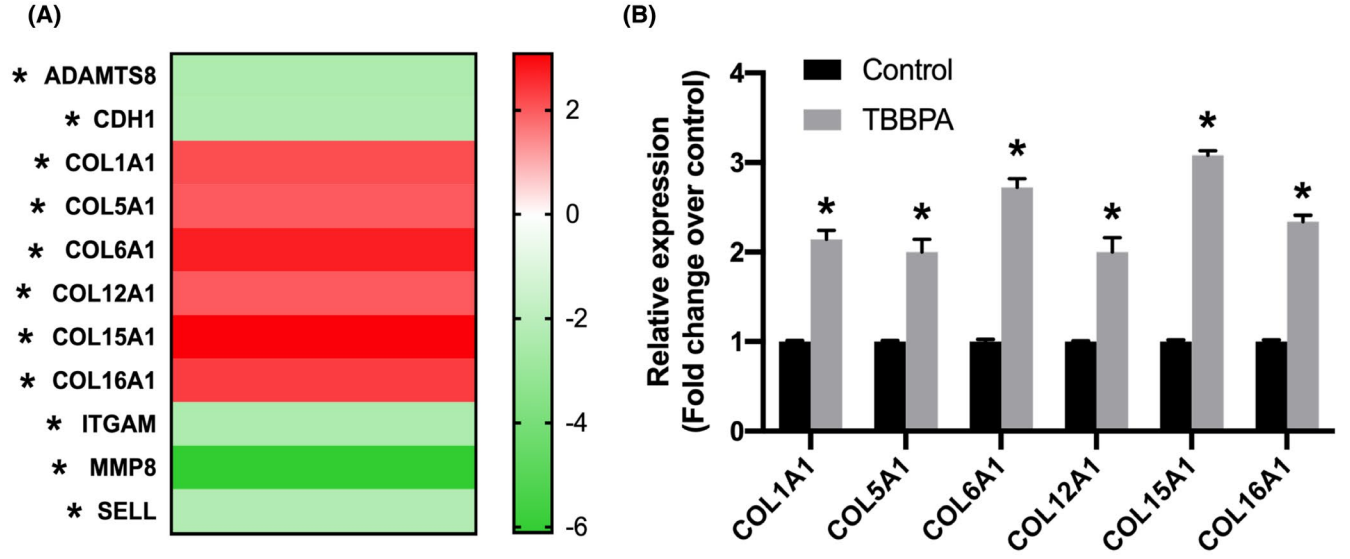

FIGURE 3 Extracellular matrix (ECM) gene expression in 3D ht-UtLM spheroids treated with TBBPA at 10^{-3} μM for 24 h. ECM gene expression was assessed by ECM RT^2 profiler PCR array. (A) Heat map of significantly regulated ECM genes, upregulated (Red) or downregulated (Green). Fold regulation cutoff: 2, and *p*-value cutoff: .05. (B) Differentially regulated expression of collagens mRNA. *$p < .05$ compared to control

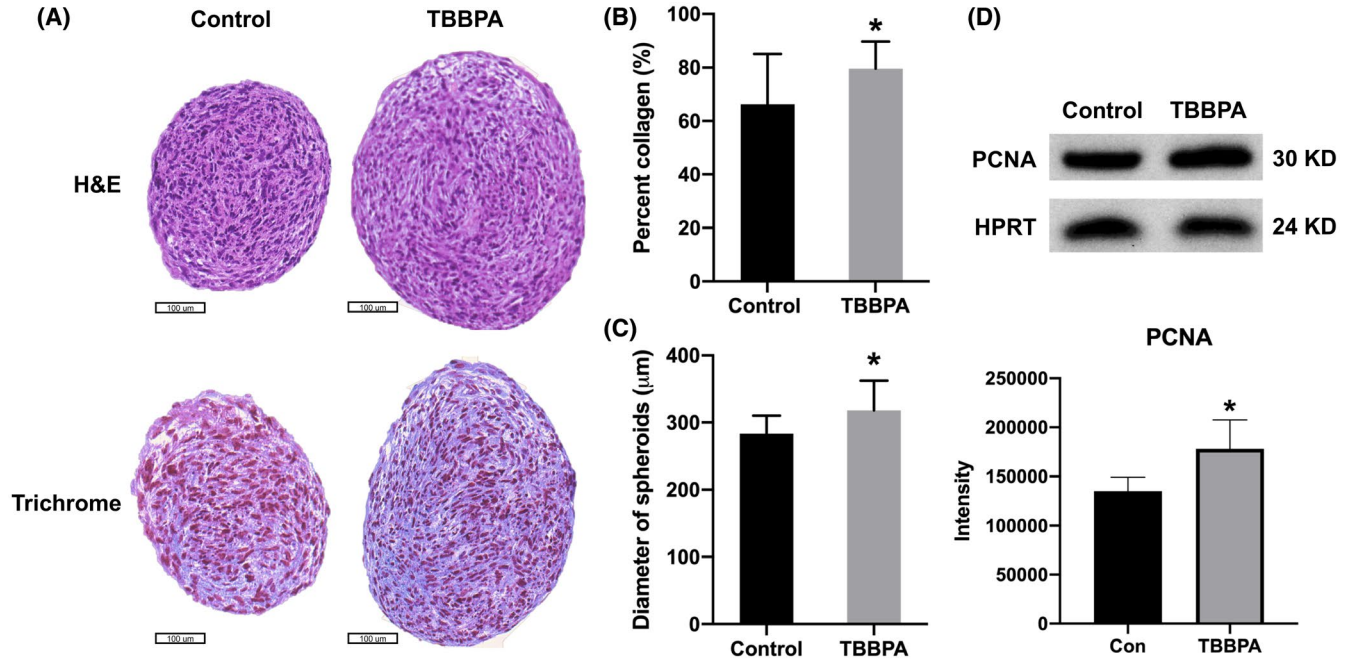

FIGURE 4 Collagen accumulation in 3D ht-UtLM spheroids treated with TBBPA for 7 days. (A) Hematoxylin and eosin (H&E) staining (top) and Masson's Trichrome staining (bottom). (B) Quantification of collagen content (blue). (C) Diameter of spheroids. *$p < .05$ compared to control. (D) PCNA expression and intensity quantification by western blotting. Scale bar = 100 μm

3.4 | Mechanisms of profibrotic effect induced by TBBPA on fibrosis-associated genes expression in 3D ht-UtLM spheroids

To further investigate the mechanisms of profibrotic effects in uterine fibroids, Fibrosis RT^2 PCR arrays were used to evaluate the status of differentially expressed genes associated with fibrosis induced by TBBPA at 24 h. There were 56 genes significantly regulated by TBBPA (Figure S2a) ($p < .05$). Outcomes from PCR arrays were subjected to IPA canonical signaling pathways analysis. The top 10 enriched canonical signaling pathways were TGFB signaling,

integrin signaling, p38 MAPK signaling, PPARα/RXRα activation, PTEN signaling, IL-8 signaling, IL-6 signaling, BMP signaling, PPAR signaling, and PI3K/AKT signaling (Figure S2b). IPA predicted the activation or inhibition of these pathways based on *z* scores represented in orange or blue color, respectively. The main activated canonical pathways induced by TBBPA were TGFB and integrin signaling pathways, which both are well known for playing a key role in the induction of fibrosis when activated.[29]

Upstream analysis by IPA was used to predict the upstream transcriptional regulators and downstream functions in TBBPA-treated ht-UtLM spheroids. An overlap *p*-value was computed based on significant overlap between genes in the dataset and known targets of the transcriptional regulators in Ingenuity Pathway Knowledge Base. The activation *z*-score algorithm was used to make predictions. IPA predicted TBBPA-induced activation of upstream regulator TGFB1 (activation *z*-score 2.608, overlap *p*-value 6.38E−73). In the TGFB1 network, *TGFB1* was predicted to be a hub gene, and upregulated genes were labeled red, while downregulated genes were green (Figure 5A). Among these genes, the key molecules including TGFB ligands (*TGFB1*, *TGFB3*) and its receptor *TGFBR1*, as well as downstream molecules SMADs (*SMAD3*, *SMAD4*) were all upregulated significantly (fold change >2 and $p < .05$) (Figure 5B), predicting the activation of TGFB signaling.

Further upstream functional analysis examined the potential functions of TBBPA-activated TGFB1 network. There were 39 genes in this network associated with fibrosis (*p*-value 1.87E−45), and 25 of these genes with red relationship lines between TGFB1 network and fibrosis were predicted to be activated (Figure 6). There were 24 genes related to proliferation of smooth muscle cells (*p*-value 2.35E−30), and 22 of them with red lines predicted activation of proliferation of smooth muscle cells (Figure 6). In combination with the canonical pathway analysis above, it suggested that TBBPA might activate cell proliferation and fibrosis functions in ht-UtLM spheroids through TGFB signaling.

3.5 | Activation of TGFB signaling proteins in 3D ht-UtLM spheroids induced by TBBPA

With the prediction of activation of TGFB signaling from the Fibrosis RT² PCR array, a TGFB phospho-protein

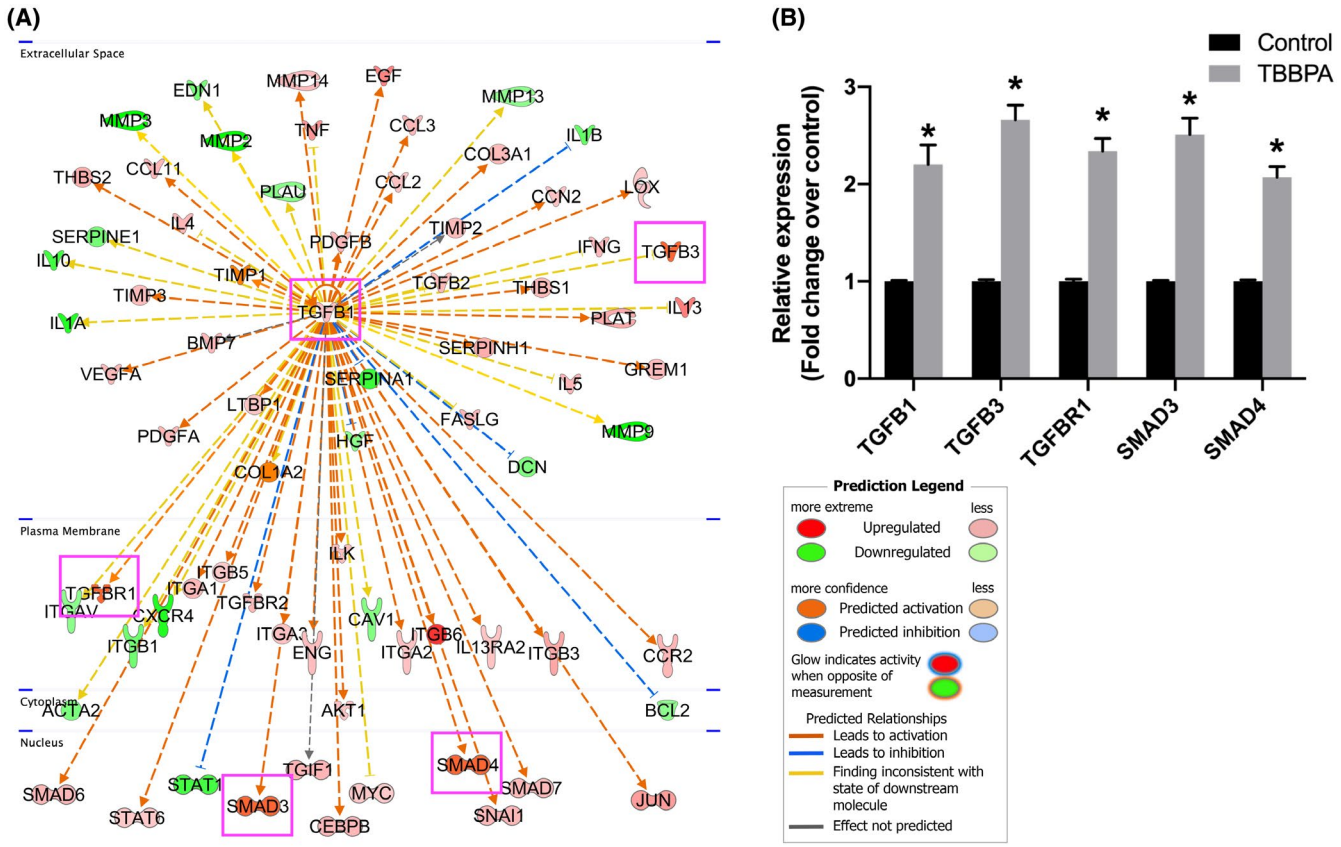

FIGURE 5 Upstream analysis of Fibrosis RT² profiler PCR array in 3D ht-UtLM spheroids induced by TBBPA at 24 h. (A) Upstream regulators analysis predicting the activation of TGFB signaling through the TGFB1 network. Upregulated genes are labeled red, and downregulated genes are labeled green. (B) Differentially expressed genes associated with TGFB signaling. *$p < .05$ compared to control

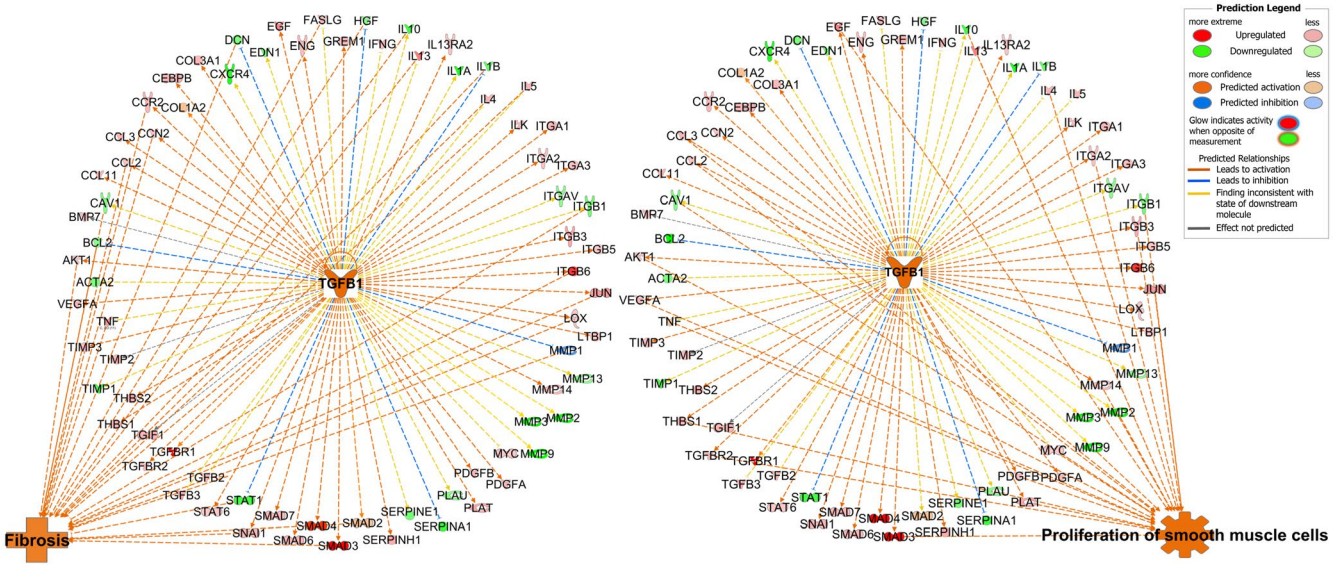

FIGURE 6 Upstream functional analysis of TBBPA-activated TGFB1 network in Fibrosis RT^2 profiler PCR array. The red relationship lines between TGFB1 network and organization of ECM predicted activation

array was then conducted to further explore the role of TGFB signaling on fibrosis in 3D ht-UtLM spheroids at the protein level. The TGFB phospho-protein array contained 176 specific phosphorylation antibodies for the TGFB signaling pathway. It was conducted at 3 h after TBBPA treatment and the data were analyzed by IPA. IPA upstream regulators analysis showed three upstream regulators were predicted to be activated with TBBPA treatment, TGFB1 (activation *z*-score 2.271, overlap *p*-value 1.52E−16), TGFBR1 (activation *z*-score 2.372, overlap *p*-value 3.01E−12), and TGFBR2 (activation *z*-score 2.161, overlap *p*-value 6.01E−08) (Figure S3a–c). In these three networks, differentially phosphorylated proteins were labeled in colors, with red indicating increased and green indicating decreased protein expression levels. Among these proteins, the key molecules typical of TGFB signaling included the TGFB ligand (TGFB1) and its receptor (TGFBR1), as well as downstream proteins SMADs (SMAD2/3) were significantly expressed in TBBPA-treated spheroids compared to the controls (fold change >1.5, $p < .05$) (Figure S3d). This implied the activation of typical TGFB/SMAD signaling. The activated phosphorylation residues for SMADs were SMAD2/3 (Thr-8), SMAD3 (Ser204), and SMAD3 (Thr179) (Figure S3d), which have been reported to be associated with hepatic fibrogenesis or myocardial fibrosis.[30,31]

Further function analysis of the three combined networks of protein expression data was conducted to investigate their association with fibrosis. There were 10 proteins associated with fibrogenesis, eight of which have red relationship lines predicted the activation of fibrogenesis, including the TGFB1 ligand and its receptors, TGFBR1 and TGFBR2, as well as MAP2K6, MAPK8, CFL1, SMAD2, and SMAD3 as downstream molecules (Figure 7). This demonstrates that TBBPA could activate fibrogenesis in ht-UtLM spheroids through TGFB signaling and increased the induction of several profibrotic proteins. The further canonical pathway analysis predicted the activation of TGFB signaling. In TGFB signaling, TGFB ligands bound to a receptor complex consisting of TGFBR2 and TGFBR1 components, and then induced the phosphorylation of receptor TGFBR1. The activated TGFBR1 then phosphorylated the downstream effectors SMAD2 and SMAD3, which complexed with Smad4 to translocate to the nucleus and regulate the expression of genes associated with fibrosis (Figure 8). All the above demonstrated the pivotal role of TGFB signaling in fibrosis of uterine fibroid 3D spheroids induced by TBBPA.

4 | DISCUSSION

Fibrosis is the common outcome observed in uterine fibroids, characterized by the excessive accumulation of ECM components. Due the high incidence of fibroids and with hysterectomy being the only essential curative treatment,[21] it is critical to investigate the mechanisms of uterine fibroid development and explore the potential role of how environmental exposures might contribute to this process. Also, to address replacement, reduction, and refinement efforts in biomedical research, there has been a focus to decrease the use of animals. Therefore, it is necessary to explore in vitro models that closely mimic in vivo tumors in humans to understand the mechanisms of progression of human disease processes.

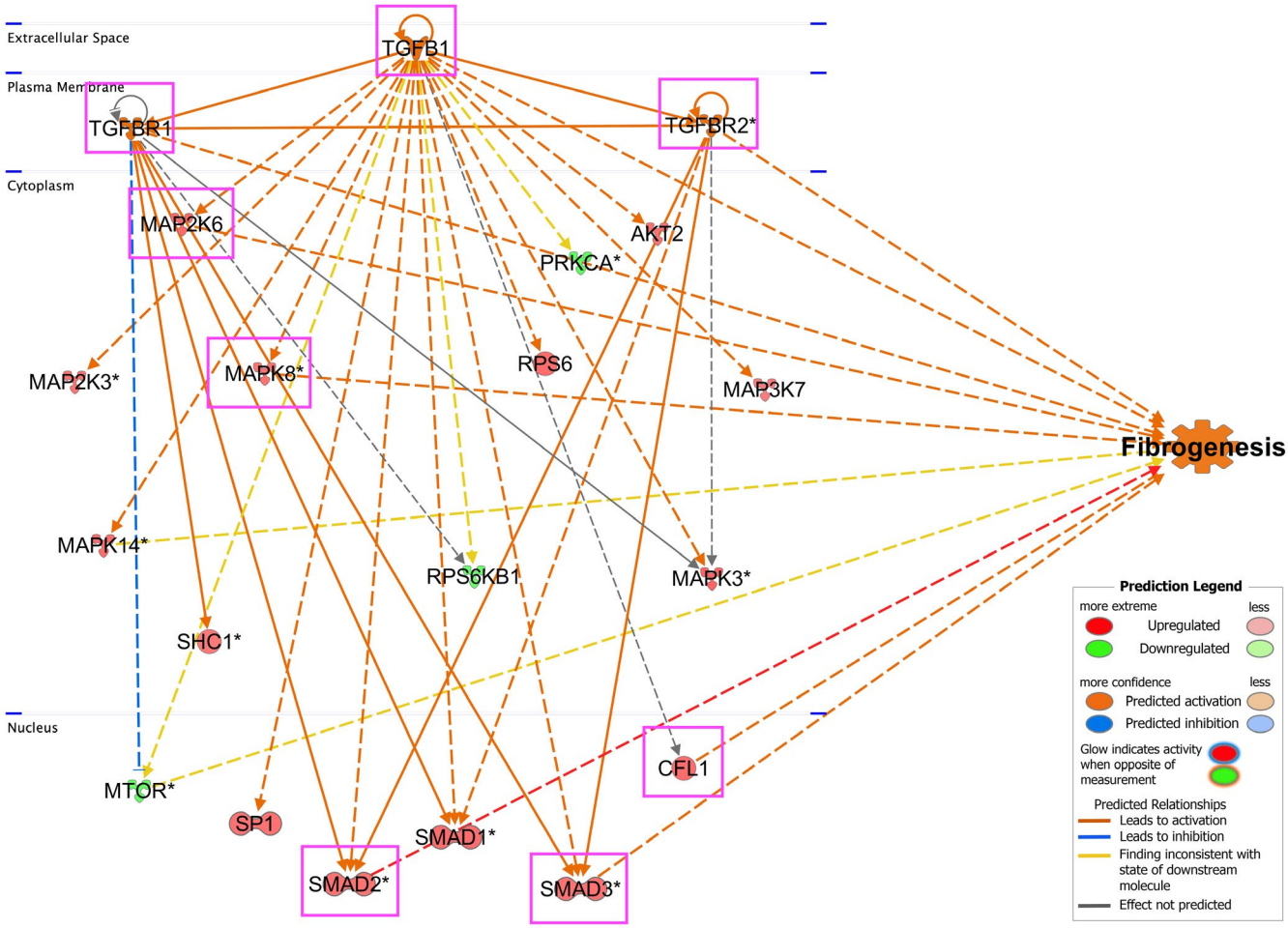

FIGURE 7 Function analysis for networks of TGFB1, TGFBR1, and TGFBR2. The data of TGFB phospho-protein array were analyzed by IPA in 3D ht-UtLM spheroids with TBBPA treatment at 3 h. The red relationship lines between molecules in the networks and function predicted the activation of fibrogenesis

For in vitro models, 2D culture systems have been used for years, but may be limited in their representation of the physiological capabilities of the microenvironment of living organisms.[32] Therefore, we developed a 3D culture system of immortalized ht-UtLM cells to study the effects of TBBPA on fibrosis, which better mimics the signaling, growth, and diffusion conditions found in uterine fibroids in vivo. One main concern for immortalized cells is that they do not completely mimic the natural life of primary cells because of their unlimited replication ability. Most primary cells possess a limited proliferation potential and undergo senescence.[33] Primary 3D fibroid spheroids have been previously established to analyze the senescence and senolytic phenotypes in uterine leiomyoma.[23] The genetic characteristics and age of the donors are also important, as the cells can behave differently under the same culture conditions. Immortalized cells, however, offer several advantages, such as cost effectiveness, easy to use, unlimited supply of material, can bypass ethical concerns associated with the use of human tissue, and a pure population of a specific cell type of interest without the concern of contamination by unwanted cells, which provides a consistent sample and reproducible results.

To investigate the effects of TBBPA on fibrosis in uterine fibroid 3D cultures, we chose TBBPA concentrations relevant to human population exposure levels. TBBPA has been detected in almost all environmental compartments and biotic samples worldwide, rendering it a ubiquitous contaminant. Kicinski et al.[27] found that the level of TBBPA in the serum of 515 high school students in Belgium ranged from <0.015 to 0.186 μg/L, which was estimated to be about 10^{-3} μM/L. In an infant–mother paired study in Korea, TBBPA concentration in mothers' serum ranged at 0.05–74 ng/g lipid weight, while the infants had higher levels of 0.05–713 ng/g lipid weight.[5] Higher levels in the infants were thought to occur due to high maternal TBBPA transfer efficiency with immature metabolic capabilities of infants leading to the accumulation of TBBPA. In addition, many studies in the United States, France, Japan, and China have tested TBBPA in human milk, ranging from <0.03 to 37.3 ng/g lipid weight.[6] Therefore, in this study, we treat the ht-UtLM spheroids with TBBPA

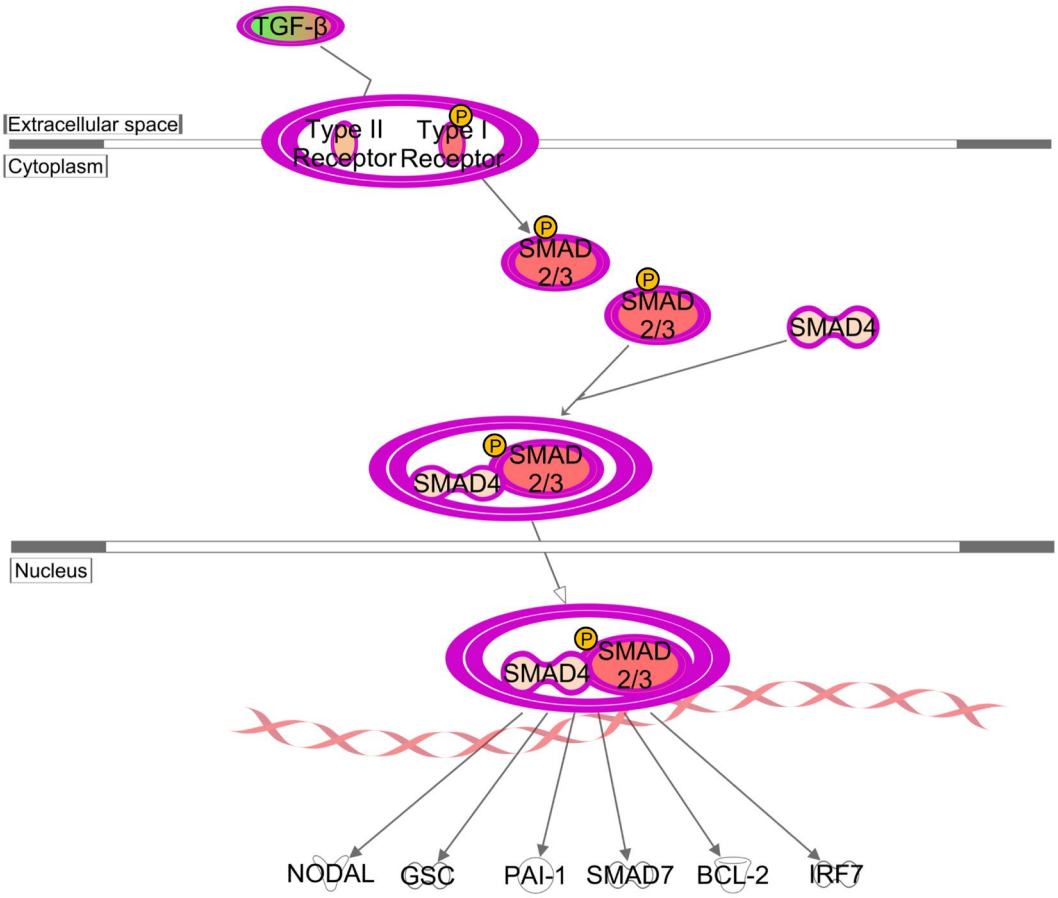

FIGURE 8 Activation of TGFB/SMAD signaling pathway induced by TBBPA in 3D ht-UtLM spheroids at the protein level. TGF-β phospho-protein array was assessed at 3 h after treatment and analyzed by IPA. TGFB bound to the receptor complex and subsequently phosphorylated TGFBR1, which in turn phosphorylated SMAD2 and SMAD3. SMAD4 then bound to p-SMAD2/3 and translocated to the nucleus to transcribe genes regulating fibrosis or early development

at a dose of 10^{-3} μM, which has a significant effect on cell proliferation and fibrosis and is also relevant to exposure levels observed in the general population. Further research is required to evaluate the occupational exposures of TBBPA at work sites to get an accurate risk assessment for TBBPA. Additionally, TBBPA is rapidly metabolized in mammals, with the estimated half-life in rats less than 3 days.[3] TBBPA-glucuronide and -sulfate are the major metabolites in blood and urine of human and rats.[34,35] Their bioaccumulation properties and potential toxicity, particularly the endocrine disruption effects, have garnered extensive attention. However, the toxicity of TBBPA and its metabolites remains controversial.[36–39] So far, there are few studies addressing the potential risk of these metabolites on the induction of fibrotic diseases. More effective strategies for evaluating TBBPA and its metabolites for their fibrotic effects are needed.

In this study, we found that many subtypes of collagen genes (*COL1A1*, *COL5A1*, *COL6A1*, *COL12A1*, *COL15A1*, and *COL16A1*) were upregulated by TBBPA administration, and the increased accumulation of collagen proteins were observed in ht-UtLM spheroids treated with TBBPA. This indicates that TBBPA can promote collagen production and accumulation in uterine fibroid spheroids. The analyses of Fibrosis RT^2 profiler arrays demonstrated the upregulation of typical TGFB pathway genes (*TGFB1*, *TGFB3*, *TGFBR1*, *SMAD3*, and *SMAD4*) with consistent results of these proteins confirmed in TGFB phospho-protein arrays. Further analyses by IPA predicted the activation of the TGFB signaling pathway at both the gene and phospho-protein levels. All these findings demonstrate the profibrotic effects of TBBPA in human uterine fibroid spheroids through TGFB signaling pathway.

TGFB pathway is widely recognized as a core pathway of fibrosis and also in the excessive ECM production often observed in fibroids.[40] In TGFB signaling, members of the TGFB superfamily are the primary factors that drives fibrosis in many fibrotic diseases.[41] Three TGFB isoforms (TGFB1, TGFB2, and TGFB3) have been identified in mammals, which share 70%–82% homology at the amino acid level.[42] In women with uterine fibroids, TGFB1 and TGFB3 have been shown expressed increasingly in fibroids

compared to the normal smooth muscles.[43] In this study, TGFB1 appears to be the most relevant isoform. With exposure to TBBPA, TGFB1 was significantly increased in ht-UtLM spheroids to drive the induction of fibrosis.

In most fibrotic diseases, TGFB elicits signaling through a SMAD-dependent pathway,[44] leading to excessive production of ECM and inhibition of ECM degradation. The canonical TGFB/SMAD signaling pathway involves the ligands TGFB, its receptor TGFBR1 and TGFBR2, as well as SMAD family proteins. SMADs can be grouped into three functional classes: the receptor-regulated SMADs (R-SMADs, SMAD1, 2, 3, 5, and 8), the common mediator SMADs (Co-SMAD and SMAD4), and the inhibitory SMADs (I-SMADs, SMAD6 and 7).[44] This study demonstrated that TBBPA administration induced ECM deposition in 3D uterine leiomyoma spheroids through the canonical TGFB/SMAD pathway: TBBPA induced overexpression of TGFB1, which bound to the receptor complex TGFBR2 and TGFBR1, and subsequently phosphorylated TGFBR1, which in turn phosphorylated R-SMADs (SMAD2 and SMAD3). Co-SMAD (SMAD4) then bound to p-SMAD2/3 and translocated to the nucleus to transcribe genes regulating fibrosis.

In addition to a SMAD-dependent pathway, TGFB may also elicit signaling through SMAD-independent pathways, such as MAPK pathway, PI3K/Akt, and Wnt and Notch signaling cascades.[45] Whether TBBPA can induce fibrosis through noncanonical pathways needs further investigation. Next, we will focus on studying the molecular mechanisms of fibrosis induction by TBBPA and confirming TGFB pathway involvement by using pathway-selective inhibitors, as well as evaluating the cross talk between SMAD-dependent and -independent pathways.

In conclusion, this study demonstrates that a human ht-UtLM 3D culture system is an effective model for studying fibrosis in human uterine leiomyomas in response to environmental exposures. TBBPA can promote fibrosis in ht-UtLM 3D cultures through a canonical TGFB/SMAD signaling pathway, which could possibly pose a health risk to women exposed to TBBPA or other profibrotic environmental contaminants.

ACKNOWLEDGMENTS

The authors thank Drs. Erin Quist and Jianping (Jim) Xue for their critical review of this manuscript, and Lois S. Wyrick for her help in organizing the figures. This work was supported by the Intramural Research Program of the NIH, NIEHS, and DNTP (ES021196-27).

DISCLOSURES

The authors declared no potential conflict of interest for the research, authorship, and publication of this article.

AUTHOR CONTRIBUTIONS

Jingli Liu designed and performed the research, analyzed the data, and wrote the manuscript; Linda Yu, Lysandra Castro, Yitang Yan, and Natasha P. Clayton performed the research; Pierre Bushel, Norris D. Flagler, and Erica Scappini analyzed the data; and Darlene Dixon designed the research and revised the manuscript.

ORCID

Darlene Dixon https://orcid.org/0000-0002-7001-2985

REFERENCES

1. Yu Y, Yu Z, Chen H, et al. Tetrabromobisphenol A: disposition, kinetics and toxicity in animals and humans. *Environ Pollut*. 2019;253:909-917.
2. Bastos PM, Eriksson J, Green N, Bergman A. A standardized method for assessment of oxidative transformations of brominated phenols in water. *Chemosphere*. 2008;70:1196-1202.
3. Hakk H, Letcher RJ. Metabolism in the toxicokinetics and fate of brominated flame retardants—a review. *Environ Int*. 2003;29:801-828.
4. Howard PH, Muir DC. Identifying new persistent and bioaccumulative organics among chemicals in commerce. III: byproducts, impurities, and transformation products. *Environ Sci Technol*. 2013;47:5259-5266.
5. Kim UJ, Oh JE. Tetrabromobisphenol A and hexabromocyclododecane flame retardants in infant-mother paired serum samples, and their relationships with thyroid hormones and environmental factors. *Environ Pollut*. 2014;184:193-200.
6. Abou-Elwafa Abdallah M. Environmental occurrence, analysis and human exposure to the flame retardant tetrabromobisphenol-A (TBBP-A)—a review. *Environ Int*. 2016;94:235-250.
7. Kitamura S, Suzuki T, Sanoh S, et al. Comparative study of the endocrine-disrupting activity of bisphenol A and 19 related compounds. *Toxicol Sci*. 2005;84:249-259.
8. Samuelsen M, Olsen C, Holme JA, Meussen-Elholm E, Bergmann A, Hongslo JK. Estrogen-like properties of brominated analogs of bisphenol A in the MCF-7 human breast cancer cell line. *Cell Biol Toxicol*. 2001;17:139-151.
9. Li J, Ma M, Wang Z. In vitro profiling of endocrine disrupting effects of phenols. *Toxicol In Vitro*. 2010;24:201-207.
10. Lyche JL, Rosseland C, Berge G, Polder A. Human health risk associated with brominated flame-retardants (BFRs). *Environ Int*. 2015;74:170-180.
11. Yu Y, Xiang M, Gao D, et al. Absorption and excretion of Tetrabromobisphenol A in male Wistar rats following subchronic dermal exposure. *Chemosphere*. 2016;146:189-194.
12. Dunnick JK, Sanders JM, Kissling GE, Johnson CL, Boyle MH, Elmore SA. Environmental chemical exposure may contribute to uterine cancer development: studies with tetrabromobisphenol A. *Toxicol Pathol*. 2015;43:464-473.
13. NTP. *Technical Report on the Toxicology Studies of Tetrabromobisphenol A (CASNO. 79-94-7) in F344/NTac Rats and B6C3F1/N Mice and Toxicology and Carcinogenesis Study of Tetrabromobisphenol A in Wistar Han [Crl: WI (Han)] Rats and B6C3F1/N Mice (Gavage Studies)*. National Toxicology Program. Accessed December 22, 2021. https://ntp.niehs.nih.gov/ntp/htdocs/lt_rpts/tr587_508.pdf

14. Kendziorski JA, Belcher SM. Strain-specific induction of endometrial periglandular fibrosis in mice exposed during adulthood to the endocrine disrupting chemical bisphenol A. *Reprod Toxicol*. 2015;58:119-130.
15. Newbold RR, Jefferson WN, Padilla-Banks E. Long-term adverse effects of neonatal exposure to bisphenol A on the murine female reproductive tract. *Reprod Toxicol*. 2007;24:253-258.
16. Hu Y, Zhang L, Wu X, et al. Bisphenol A, an environmental estrogen-like toxic chemical, induces cardiac fibrosis by activating the ERK1/2 pathway. *Toxicol Lett*. 2016;250-251:1-9.
17. Elswefy SE, Abdallah FR, Atteia HH, Wahba AS, Hasan RA. Inflammation, oxidative stress and apoptosis cascade implications in bisphenol A-induced liver fibrosis in male rats. *Int J Exp Pathol*. 2016;97:369-379.
18. Evans P, Brunsell S. Uterine fibroid tumors: diagnosis and treatment. *Am Fam Physician*. 2007;75:1503-1508.
19. Stewart EA, Laughlin-Tommaso SK, Catherino WH, Lalitkumar S, Gupta D, Vollenhoven B. Uterine fibroids. *Nat Rev Dis Primers*. 2016;2:16043.
20. Baird DD, Dunson DB, Hill MC, Cousins D, Schectman JM. High cumulative incidence of uterine leiomyoma in black and white women: ultrasound evidence. *Am J Obstet Gynecol*. 2003;188:100-107.
21. Sabry M, Al-Hendy A. Medical treatment of uterine leiomyoma. *Reprod Sci*. 2012;19:339-353.
22. Carney SA, Tahara H, Swartz CD, et al. Immortalization of human uterine leiomyoma and myometrial cell lines after induction of telomerase activity: molecular and phenotypic characteristics. *Lab Invest*. 2002;82:719-728.
23. Xie J, Xu X, Yin P, et al. Application of ex-vivo spheroid model system for the analysis of senescence and senolytic phenotypes in uterine leiomyoma. *Lab Invest*. 2018;98:1575-1587.
24. Clayton NP, Burwell A, Jensen H, et al. Preparation of three-dimensional (3-D) human liver (HepaRG) cultures for histochemical and immunohistochemical staining and light microscopic evaluation. *Toxicol Pathol*. 2018;46:653-659.
25. Flake GP, Moore AB, Flagler N, et al. The natural history of uterine leiomyomas: morphometric concordance with concepts of interstitial ischemia and inanosis. *Obstet Gynecol Int*. 2013;2013:285103.
26. Flake GP, Moore AB, Sutton D, et al. The life cycle of the uterine fibroid myocyte. *Curr Obstet Gynecol Rep*. 2018;7:97-105.
27. Kicinski M, Viaene MK, Den Hond E, et al. Neurobehavioral function and low-level exposure to brominated flame retardants in adolescents: a cross-sectional study. *Environ Health*. 2012;11:86.
28. Lu P, Takai K, Weaver VM, Werb Z. Extracellular matrix degradation and remodeling in development and disease. *Cold Spring Harb Perspect Biol*. 2011;3:a005058.
29. Song KH, Cho SJ, Song JY. Alphavbeta1 integrin as a novel therapeutic target for tissue fibrosis. *Ann Transl Med*. 2016;4:411.
30. Farini A, Villa C, Di Silvestre D, et al. PTX3 predicts myocardial damage and fibrosis in duchenne muscular dystrophy. *Front Physiol*. 2020;11:403.
31. Yoshida K, Matsuzaki K, Murata M, Yamaguchi T, Suwa K, Okazaki K. Clinico-pathological importance of TGF-beta/phospho-smad signaling during human hepatic fibrocarcinogenesis. *Cancers*. 2018;10:183.
32. Edmondson R, Broglie JJ, Adcock AF, Yang L. Three-dimensional cell culture systems and their applications in drug discovery and cell-based biosensors. *Assay Drug Dev Technol*. 2014;12:207-218.
33. Hayflick L, Moorhead PS. The serial cultivation of human diploid cell strains. *Exp Cell Res*. 1961;25:585-621.
34. Knudsen GA, Sanders JM, Sadik AM, Birnbaum LS. TITLE disposition and kinetics of tetrabromobisphenol A in female Wistar Han rats. *Toxicol Rep*. 2014;1:214-223.
35. Schauer UM, Volkel W, Dekant W. Toxicokinetics of tetrabromobisphenol a in humans and rats after oral administration. *Toxicol Sci*. 2006;91:49-58.
36. Fini JB, Riu A, Debrauwer L, et al. Parallel biotransformation of tetrabromobisphenol A in *Xenopus laevis* and mammals: *Xenopus* as a model for endocrine perturbation studies. *Toxicol Sci*. 2012;125:359-367.
37. McCormick JM, Paiva MS, Haggblom MM, Cooper KR, White LA. Embryonic exposure to tetrabromobisphenol A and its metabolites, bisphenol A and tetrabromobisphenol A dimethyl ether disrupts normal zebrafish (*Danio rerio*) development and matrix metalloproteinase expression. *Aquat Toxicol*. 2010;100:255-262.
38. Debenest T, Gagne F, Petit AN, Andre C, Kohli M, Blaise C. Ecotoxicity of a brominated flame retardant (tetrabromobisphenol A) and its derivatives to aquatic organisms. *Comp Biochem Physiol C Toxicol Pharmacol*. 2010;152:407-412.
39. Akiyama E, Kakutani H, Nakao T, et al. Facilitation of adipocyte differentiation of 3T3-L1 cells by debrominated tetrabromobisphenol A compounds detected in Japanese breast milk. *Environ Res*. 2015;140:157-164.
40. Györfi AH, Matei A-E, Distler JHW. Targeting TGF-β signaling for the treatment of fibrosis. *Matrix Biol*. 2018;68-69:8-27.
41. Frangogiannis N. Transforming growth factor-beta in tissue fibrosis. *J Exp Med*. 2020;217:e20190103.
42. Meng XM, Nikolic-Paterson DJ, Lan HY. TGF-beta: the master regulator of fibrosis. *Nat Rev Nephrol*. 2016;12:325-338.
43. Ciebiera M, Wlodarczyk M, Wrzosek M, et al. Role of transforming growth factor beta in uterine fibroid biology. *Int J Mol Sci*. 2017;18:2435.
44. Biernacka A, Dobaczewski M, Frangogiannis NG. TGF-beta signaling in fibrosis. *Growth Factors*. 2011;29:196-202.
45. Derynck R, Zhang YE. Smad-dependent and Smad-independent pathways in TGF-beta family signalling. *Nature*. 2003;425:577-584.

SUPPORTING INFORMATION

Additional supporting information may be found in the online version of the article at the publisher's website.

How to cite this article: Liu J, Yu L, Castro L, et al. Short-term tetrabromobisphenol A exposure promotes fibrosis of human uterine fibroid cells in a 3D culture system through TGF-beta signaling. *FASEB J*. 2022;36:e22101. doi:10.1096/fj.202101262R